INVESTIGATION OF THE INLET FILTER INFLUENCE ON UNSTEADY FLOW PHENOMENA IN A SINGLE-STAGE CENTRIFUGAL BLOWER

K. Kabalyk, W. Kryłłowicz, G. Liśkiewicz, L. Horodko

Lodz University of Technology, Institute of Turbomachinery, Lodz, Poland,
kirill.kabalyk@p.lodz.pl

ABSTRACT

The instantaneous static pressure signal has been recorded alongside a single-stage centrifugal compressor impeller shroud tip and at the compressor outlet using four Kulite high-frequency transducers. The compressor inlet duct contained a cassette filter followed by a diagonal inlet guide. Such a design is typical for the machinery utilized for waste water aeration. The aim of the study was to check whether the filter might damp the pressure pulsations inside the compressor duct and thus decrease the unsteady aerodynamic loads on its elements. The signal analysis was held with the use of FFT-based procedure and the measurements were performed within the whole machine operational range. The experiments showed that filter disassembling caused a reasonable increase in pulsation amplitude during compressor unstable operation. The strength of the increase was found to be dependent on the inlet guide vanes setting angle. As for stable operational region, almost no differences were observed.

Key words: centrifugal compressor, inlet filter damping, unsteady flow measurements

NOMENCLATURE

A – amplitude (Pa)
D – diameter (mm)
f – frequency (Hz)
L – length (m)
$\dot{m}$ – mass flow rate (kg/s)
N – total number
n – rotor rotational speed (rpm)
Δp – static pressure difference (Pa)
TOA – throttle opening area
T – temperature (K)
u – tangential velocity (m/s)/tangential coordinate axis
z – blade number/axial coordinate axis
α_{IG} – inlet guide vane setting angle (measured from tangential direction)
β – impeller blade angle (measured from tangential direction)/orifice contraction coefficient
Π – pressure ratio
τ – time (s)

Subscripts

2 – refers to the impeller outlet
bl – blade
BP – blade passing
c – compressor
f – filter
IG – inlet guide
in – inlet
imp – impeller
max – maximal
o – orifice
out – outlet
s – surge
sample – refers to sampling parameters of the pressure transducers

INTRODUCTION

The necessity to study the aspects of unsteady aerodynamic interaction between the centrifugal compressor inlet duct elements and the compressor stage itself came from the waste water treatment industry. Several years ago some plants in Poland reported difficulties in keeping the performance of the blowers operating in waste water aeration circuit aerodynamically stable. The problems initiated after the operators started to utilize an inlet duct of a smaller volume and another filter type compared to a conventional one. The rest of the compression unit as well as the whole aeration system experienced no design alterations. Therefore, it came evident that the source of the problem should be in the inlet network design.

The search for the publications devoted to the problems of the "compressor-network" system operation mostly leads to the studies devoted to the outlet network cases (Fink, 1992, Koyama, 1955, Pfleiderer, 1998). As for the inlet network, it seems extremely difficult to retrieve any paper reporting e.g. the study of the inlet pipeline design influence on the machine performance. Due to that, a research group at the Institute of Turbomachinery, Lodz University of Technology (IMP TUL) initiated an elementary research to discover how such parameters as the inlet duct volume, inlet filter resistance, inlet guide closure etc. might affect the unsteady performance of a single stage centrifugal blower. The current paper aims to investigate the influence that a body of an inlet cassette filter might exert on the static pressure fluctuations inside the blower rotating and stationary elements.

EXPERIMENTAL TEST RIG

Test rig design description

The experimental stand meridional cross section is sketched in Fig. 1. The test rig was initially developed by Magiera (2006) and afterwards in 2013 was redesigned for the purposes of the present study (Kabalyk and Kryłłowicz, 2013). The machine is located in the Fluid Machines Laboratory of the IMP TUL. It might be classified as a low speed low pressure single stage blower due to its bounded operational impeller tip speed of $u_2 = 112\,\mathrm{m/s}$ and maximal pressure ratio of $\Pi_{c\_max} = 1.12$. The installation is compiled from the following elements (see Fig. 1):

- pos. 1 – the rectangular cross-section suction duct with a cassette type filter 600x600x200 mm in size installed inside (filled with polyester fiber);

- pos. 2 – diagonal inlet guide (IG) with a number of vanes $z_{IG} = 18$ (each vane might be rotated in accordance with or against impeller rotation);
- pos. 3 – compression stage comprising a semi-open radial swept impeller ($\beta_{bl2} = 90°$), a vaneless diffuser and an overhung volute;
- pos. 4 – discharge PVC pipeline 150 mm in diameter with a flow straightener required to deswirl the flow after the volute;
- pos. 5 – mass flow measurement orifice with a contraction coefficient of $\beta = 0.75$;
- pos. 6 – throttle valve necessary to control the mass flow through the unit.

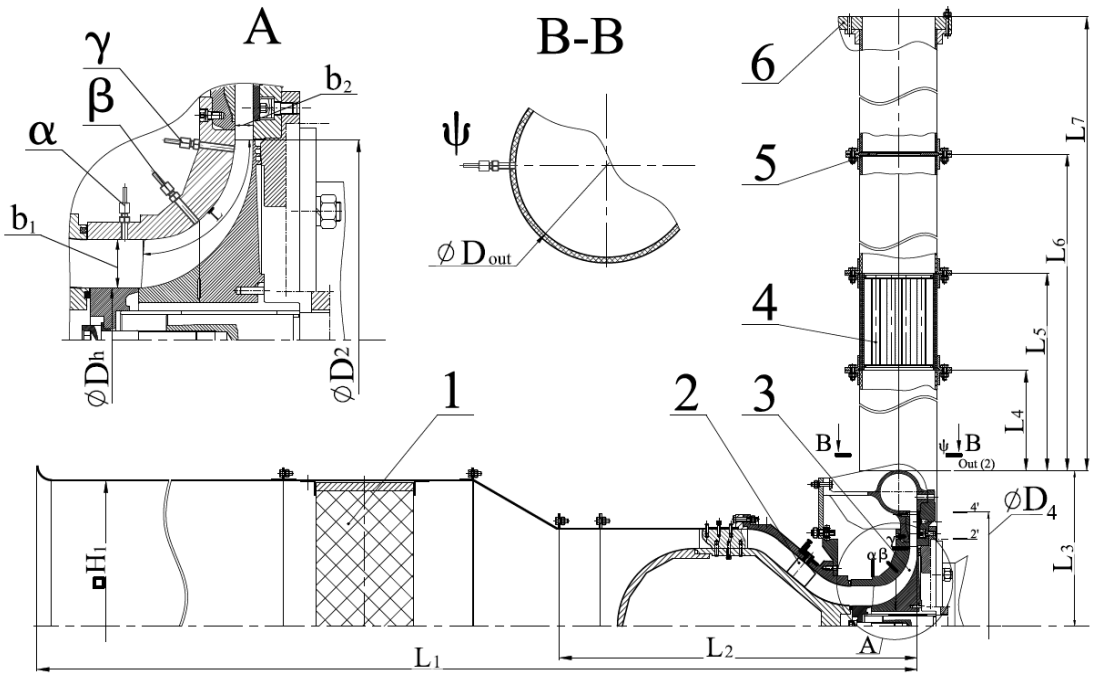

Figure 1: **Sketch of the test rig meridional cross section together with suction and discharge pipelines**

The main dimensionless geometric parameters defining the compressor rig are summarized in Tab. 1. All the values are divided by the impeller outlet diameter D_2, which is also given in the table.

The parameter of the inlet guide vane setting angle α_{IG} needs to be defined. In this work, α_{IG} is treated as the angle between the vane meanline (which is straight in our case) and the tangential direction u (see Fig. 2). The angle is positive when the vane is turned in accordance with the impeller rotational direction (positive preswirl) and has a negative value in an opposite case (negative preswirl).

Table 1: **Dimensionless values of the main geometric parameters defining the test rig**

D_2, mm	$\overline{D}_4$	$\overline{D}_h$	$\overline{D}_{out}$	$\overline{b}_1$	$\overline{b}_2$	$\overline{H}_1$
330.2	1.42	0.26	0.45	0.12	0.045	1.81
$\overline{L}_1$	$\overline{L}_2$	$\overline{L}_3$	$\overline{L}_4$	$\overline{L}_5$	$\overline{L}_6$	$\overline{L}_7$
5.81	2.24	0.97	5.61	6.21	11.1	13.5

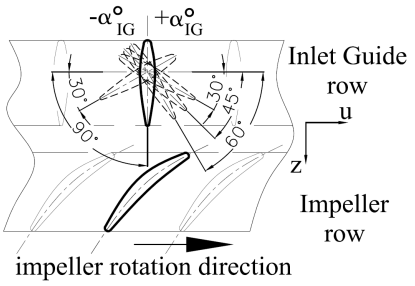

Figure 2: **Definition of the inlet guide setting angle α_{IG}**

Experimental measurements approach

To provide an assessment of the filter body effect on the blower operation it was decided to build two separate measurement systems: *steady* one for time-averaged and *unsteady* one for instantaneous pressure measurements. A schematic illustration of the way each line operates is shown in Fig. 3.

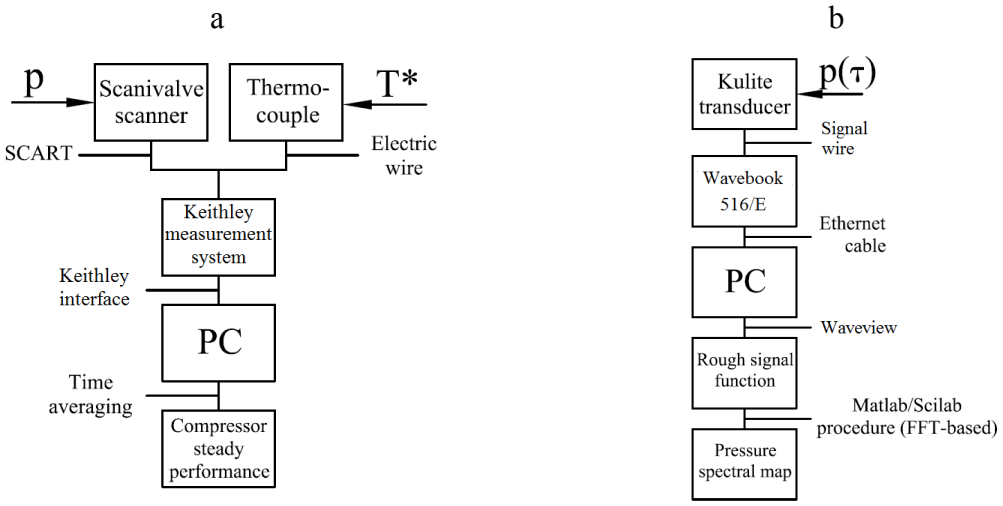

Figure 3: **Schemes of steady (a) and unsteady (b) measurement line operation**

Steady measurement line operation

The main aim of time-averaged measurements was to receive the values of such parameters as the blower static pressure rise Δp_c; static pressure drop on filter Δp_f, inlet guide Δp_{IG} and the orifice Δp_o; total temperatures at the machine inlet T_{in}^* and discharge T_{out}^* for 25 throttle positions which constituted a single test series.

Each of the pressure measurement stations represents an array of taps with diameter of 0.5 mm drilled along the duct cross section. The number of taps depends on the duct transversal size and varies from 8 to 4. The taps are connected to each other in a way to provide pneumatic averaging at every control section. A resulting "averaged" tube coming from a singular station transmits the signal to the Scanivalve scanner. The estimated measurement uncertainty error possessed by the Scanivalve is 3% of the quantity measured. The scanner does the signal averaging and moderation and sends it a PC passing a Keithley electronic system, which is necessary to couple pressure and temperature measurements. The PC displays the averaged static pressure and total temperature values making further mathematical calculations possible.

Total temperature is monitored by two thermocouples located correspondingly at the machine suction (T_{in}^*) and 200 mm upstream from the orifice (T_{out}^*).

Unsteady measurement line operation

The system was developed by Horodko, 2006, and was successfully utilized in works similar to this one and described by Liskiewicz et al., 2014, and Kabalyk et. al, 2014.

The data acquisition is based on four Kulite XCQ-093-5-psid high frequency pressure transducers positioned in a way shown in Fig. 1 (see detail "A" and section "B-B"). According to the manufacturer the transducers' measurement error constitutes 0.1% of the quantity measured. Three gauges are located along the impeller shroud correspondingly at impeller inlet ("α" gauge, $\overline{L} = -0.2$), impeller middle ("β" gauge, $\overline{L} = 0.4$) and impeller outlet ("γ" gauge, $\overline{L} = 0.9$), where $\overline{L}$ is the non-dimensional impeller blade meridional length at shroud. $\overline{L} = 0$ at the leading edge and $\overline{L} = 1$ at the trailing edge. The fourth Kulite named "ψ" is situated in the discharge pipe wall close to the volute outlet flange.

The Kulites are connected to a pressure calibrator and to a Wavebook/516E scanner via a pneumatic tube in a former and via an electric cable in a latter case. The Wavebook serves as a linking member between the gauge and the PC where Waveview software is utilized to set the gauge sampling frequency f_{sample} and signal record duration τ_{record}. Tab. 2 gives the sampling parameter set used in this work.

Table 2: **Determinative parameters of a single measurement sample**

f_{sample}, kHz	τ_{record}, s	N_{sample}
100	10.486	$2^{20} = 1048576$

After a single signal record is finished it undergoes a calibration procedure. Eventually, the resulting data array undergoes a Fast Fourier Transform (FFT) procedure to be shifted to the frequency domain. Such a treatment is applied to all the records obtained in a single series, which in case of unsteady measurements consists of 55 throttle positions from totally opened valve to its complete shutoff.

To conveniently visualize the results obtained during a test series it was decided to join the FFT spectra obtained at all valve positions into a single colour diagram that possesses pressure fluctuation frequency f along abscissa, a non dimensional parameter *Throttle Opening Area* (TOA) that defines the rate of throttling in percentage along the ordinate and the pressure fluctuation amplitude A as a colour variable.

All the data processing procedures are carried out employing either Matlab or Excel environment. The total number of test series carried out was 8: 4 series with no filter inside the inlet duct (varying the IG setting angle from $\alpha_{\text{IG}} = 90°$ to $\alpha_{\text{IG}} = 30°$) and 4 similar series with filter body present within the duct. The major trends that allow comprehending the filter body effect on the unsteady flow inside the machine are discussed in the next section.

RESULTS AND DISCUSSION

Stationary measurements

The compressor performance curves (Fig. 4,a) show a gradual shift towards the lower pressure ratios as the IG opening area decreases. Moreover, due to additional throttling outgoing from the IG the choke mass flow drops to an almost twice lower value at $\alpha_{\text{IG}} = 30°$ compared with the $\alpha_{\text{IG}} = 90°$ case. The inlet recirculation line "IR" indicates the onset of the instabilities for each performance curve. As the surge phenomenon occurred at the flow rates lower than $\dot{m} = 0.1\,\text{kg/s}$ the indication of the surge line is impossible as the orifice utilized for the mass flow measurements didn't allow to measure the flows lower than $\dot{m}_{\text{min}} = 0.174\,\text{kg/s}$.

The curves in Fig. 4,b serve to link the values of Throttle Opening Area to the corresponding mass flows $\dot{m}$. The map might be found useful when analyzing pressure fluctuation maps discussed further on as they don't provide any information concerning the mass flow but only concerning TOA.

To demonstrate the first order influence of the filter body on the installation operation the dependences of the static pressure difference Δp_{f} measured upstream and downstream the filter from the mass flow rate $\dot{m}$ are shown in the Fig. 5,a. As gets evident, the IGV positioning introduces a marginal effect on the filter pressure drop. The dependences possess almost linear character while the absolute drop value differs from $\Delta p_{\text{f\_min}} = 7.7\,\text{Pa}$ at $\dot{m} = 0.17\,\text{kg/s}$ to $\Delta p_{\text{f\_max}} = 57\,\text{Pa}$ at $\dot{m} = 1.08\,\text{kg/s}$.

In addition, Fig. 5,b illustrates the meridional velocity c_{m1} profiles measured at the impeller inlet (same location as the gauge "α") at the operating mass flow of $\dot{m} = 0.63\,\text{kg/s}$ by Magiera (Magiera, 2006). According to the graphs the throttling induced by the IGV closure reduces the mean meridional velocity level in the main stream as well as introduces a local flow acceleration close to the hub at $\alpha_{\text{IG}} = 45°$ and $\alpha_{\text{IG}} = 30°$.

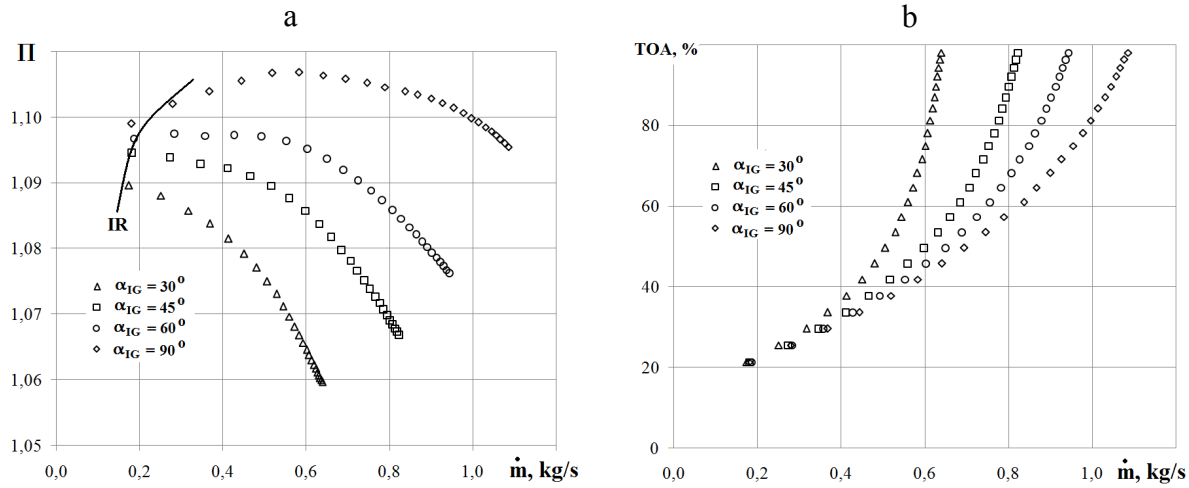

Figure 4: **Dependences of experimentally measured compressor pressure ratio Π (a) and throttle opening area TOA (b) on the mass flow rate $\dot{m}$ for the IGV setting angles α_{IG} tested**

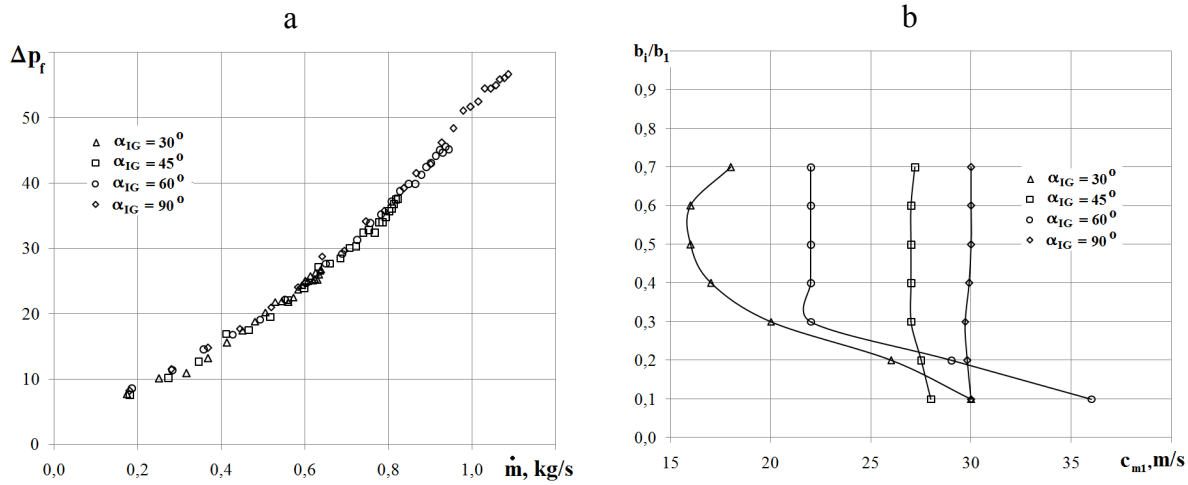

Figure 5: **Dependences of experimentally measured filter pressure drop Δp_f on the mass flow rate $\dot{m}$ (a) and experimentally measured meridional velocity c_{m1} radial profiles at impeller inlet for the IGV setting angles α_{IG} tested**

Unsteady measurements

Fully opened inlet guide

The first set of unsteady measurements results to be discussed is shown in Fig. 6. The diagrams are cut up to a half in the TOA parameter as no significant features were detected within the interval of $50\% < TOA < 100\%$ Looking at the diagrams recorded by the "α" gauge (Fig. 6,a,b) their almost absolute qualitative similarity is the first trend that gets noticeable. The interval of $27\% < TOA < 50\%$ doesn't contain any amplitude peak higher than 0.010 kPa what allows to suggest that within that region the flow stays stable. As the throttling gets higher ($15\% < TOA < 27\%$) a characteristic pseudo-sound structure (zone "A" in the Fig. 6,a) arises on both maps within the frequency region of $10^2\,\text{Hz} < f < 6 \cdot 10^3\,\text{Hz}$ and then gradually vanishes. The appearance of such zones was registered only at impeller inlet. To accurately diagnose the source that might induce such a structure a velocity radial profile at impeller inlet is to be measured. Up to this moment, the only data available is the ones shown on the Fig. 5,b that was obtained at a much higher flow rate and doesn't provide any

velocity values close to the shroud wall. However, the previous studies carried out at the same test rig (Liskiewicz and Horodko, 2014) reported that the most probable reason for such pseudo-sound area to exist must be the inception of *inlet recirculation*. This unsteady flow phenomenon is usually described as a region of separated fluid particles concentrated near the shroud wall close to the semi-open centrifugal impeller leading edge and preceding *mild* and *deep surge* (Kryllowicz, 2001). Earlier this feature was mostly reported to appear in pumps (Fraser, 1982, Yedidiah, 1996), but in recent years also has become an object of interest within centrifugal compressor researchers (Harley, 2014). Further valve closure ($0\% < \mathrm{TOA} < 10\%$) results in an emergence of a concentrated amplitude peak with a frequency of $f_s = 12.68\,\mathrm{Hz}$ (zone "B"). The peak existence is thought to signalize a *deep surge* inception. The hypothesis is based on the results of the previous studies e. g. a survey conducted by Liskiewicz (Liskiewicz and Horodko, 2014) who applied the Wavelet analysis to approve the accessory of the peak to the deep surge inception. Hence, the corresponding frequency f_s is named as the *main surge frequency*.

Qualitative comparison of the tests results at the volute outlet (Fig. 6 c,d) also detects almost no visible influence of the filter body on the fluctuation spectra. The blower stability gets weaker as throttling exceeds 80 % ($\mathrm{TOA} < 20\%$). Further TOA decrease provokes the birth of the main surge peak allocating at $f_s = 12.68\,\mathrm{Hz}$ and at least four surge modes with frequencies of $(2 \div 4) f_s$.

In spite of the results qualitative identity, taking a glance at the legends on the right hand side of each map brings to the existence of discrepancies in the amplitude maximal values. As visible, introducing a filter into the suction duct reduces the fluctuations maxima by 32% at impeller inlet and by 30% at the blower outlet.

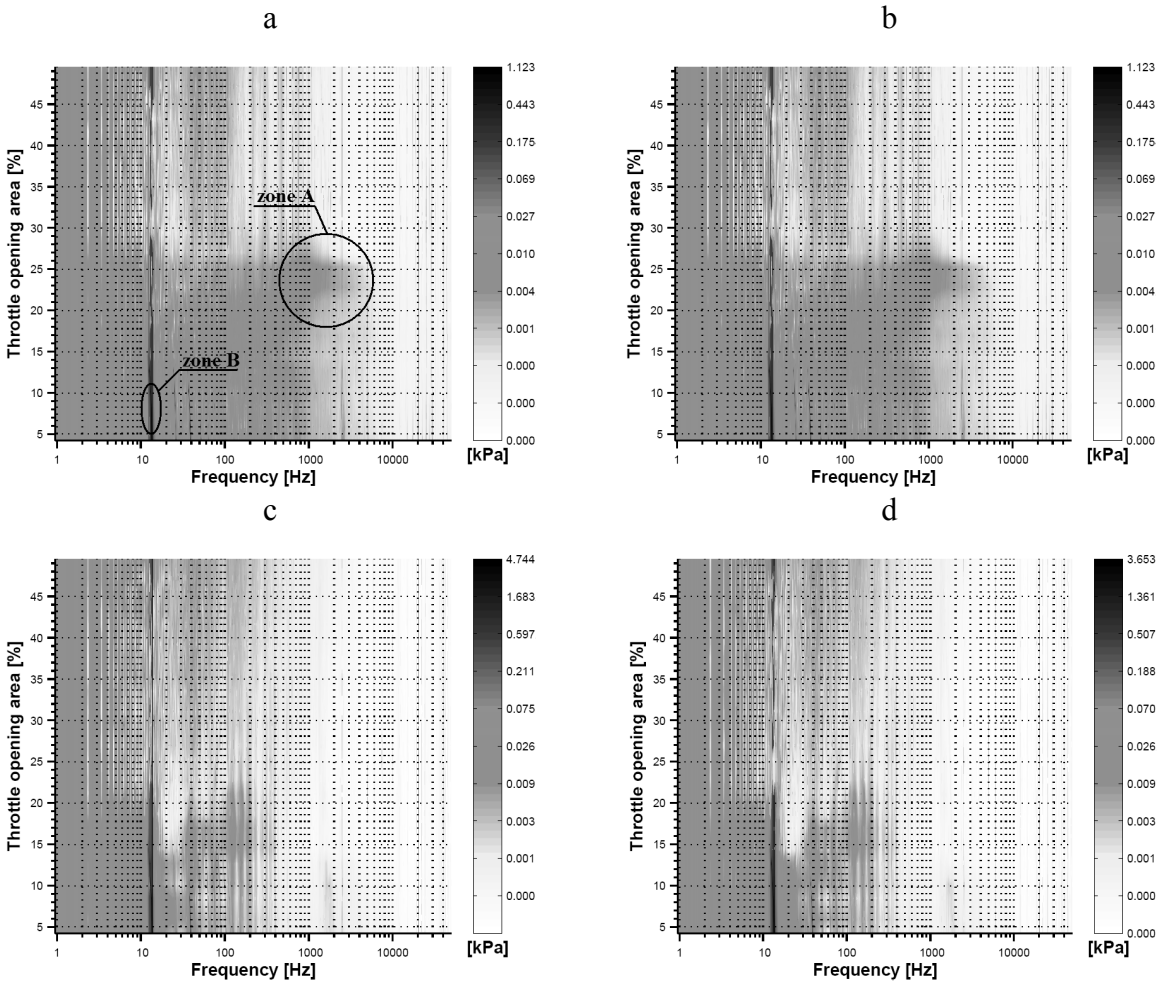

Figure 6: **Pressure fluctuation spectral maps obtained at impeller inlet (a,b) and volute outlet (c,d) without filter (left column) and with filter (right column) at** $\alpha_{IG} = 90°$

In all the cases the maxima correspond to a point of $f = f_s = 12.68\,\text{Hz}; \text{TOA} = 0\%$ what allows to name them the *main surge amplitudes* A_s. Table 3 contains the values of the amplitudes recorded at every control point.

Table 3: **Values of the main surge amplitude A_s, kPa, recorded at** $\alpha_{IG} = 90°$

Gauge	α	β	γ	ψ
No filter	1.487	1.413	0.957	4.744
Filter	1.123	1.098	0.756	3.653

To conclude with, at the fully opened IG the filter affects no influence on the fluctuation spectra inside the blower but damps the surge up to 30% of its amplitude.

Two-third opened inlet guide vane

According to the upper row of the diagrams in Fig. 7 a slight positive prewirl of the flow generated by the IG set to $\alpha_{IG} = 60°$ provokes a 4% downshift of the inlet recirculation onset after the filter is put into the duct (Fig. 7,a,b). The rest of the trends stay alike to the situation discussed above when the IG was left open. The surge frequency shows no dependence neither from the IG position nor from the filter presence/absence within the pipeline and saves the value of $f_s = 12.68\,\text{Hz}$. The filter surge damping gets stronger, though. The main surge amplitude falls by 69% at impeller inlet and by 63% at the machine discharge as the filter gets present inside the suction duct (see Tab. 4).

Table 4: **Values of the main surge amplitude A_s, kPa, recorded at** $\alpha_{IG} = 60°$

Gauge	α	β	γ	ψ
No filter	1.488	1.414	0.958	4.747
Filter	0.881	1.315	0.873	2.914

a b

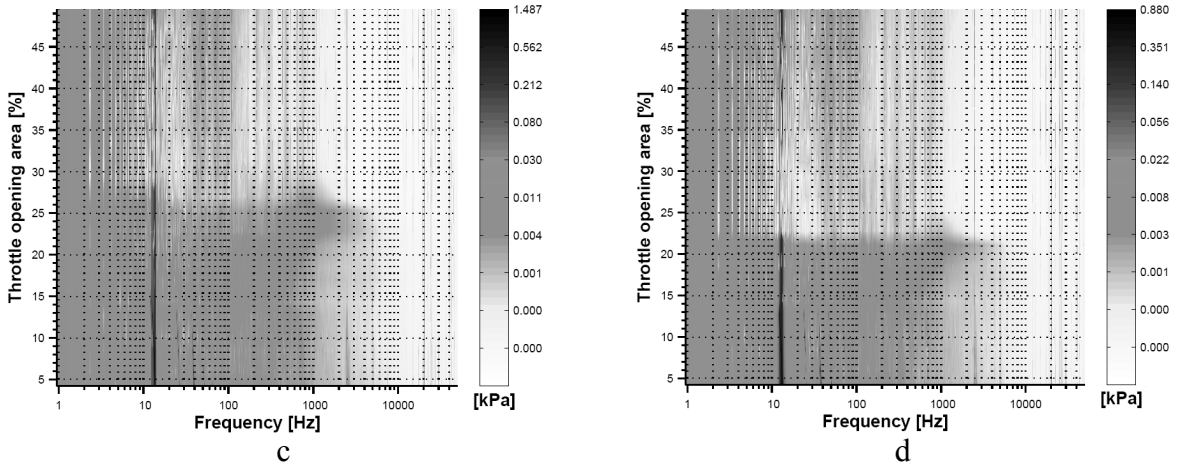

c d

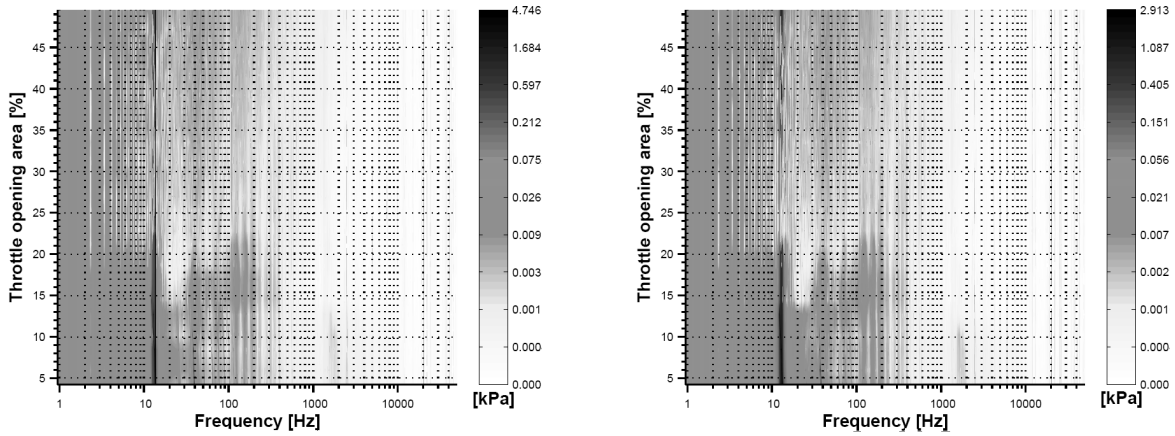

Figure 7: **Pressure fluctuation spectral maps obtained at impeller inlet (a,b) and volute outlet (c,d) without filter (left column) and with filter (right column) at** $\alpha_{IG} = 60°$

One-third opened inlet guide

The results discussed in this section were recorded at the highest rate of the IG closure possible to set at the test rig. To start with, Tab. 5 analogically to the previous cases summarizes the recorded main surge amplitude data. The highest flow deviation introduces no enhancement in filter surge damping as it was possible to expect. Oppositely, the average level of pressure pulsations even gets higher in cases when the filter body is inside. The deep surge amplitude difference almost vanishes in case of the "α" station and constitutes 8% at the impeller outlet.

Table 5: **Values of the main surge amplitude A_s, kPa, recorded at** $\alpha_{IG} = 30°$

Gauge	α	β	γ	ψ
No filter	0.901	0.953	0.908	2.277
Filter	0.901	0.992	0.983	2.358

Comparing the maps in Fig. 8 from the qualitative viewpoint a return of almost total identity in fluctuation spectra distribution might be observed. The blower aerodynamic stability margin fell to a value of $TOA = 17\%$ what is 10% lower than in case of the opened IG. In addition, it seems hard to judge whether inlet recirculation still precedes the deep surge or a higher flow prewirl eliminates any flow separations at the shroud wall up to the surge. Anyway, the presence of characteristic pseudo-sound areas earlier referred to the inlet recirculation gets much less evident.

a b

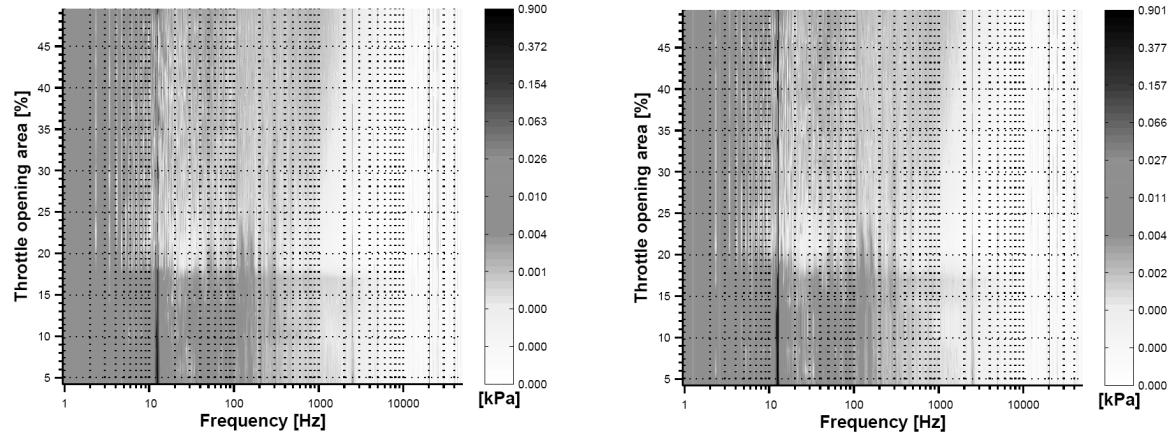

Figure 8: **Pressure fluctuation spectral maps obtained at impeller inlet (a,b) without filter (left column) and with filter (right column) at $\alpha_{IG} = 30°$**

CONCLUSIONS

The conducted study detected that the character of unsteady aerodynamic interaction between the inlet filter and a centrifugal blower stage possesses a complex nature and might depend on side factors such as IGV closure. After the performed analysis of the measurements results a following set of conclusions might be worked out.

1. The filter body installment into the duct didn't bring any qualitative or quantitative change into the character of static pressure fluctuations within the machine during its stable work. All the discovered changes concerned the blower unstable operational region.
2. The main surge frequency f_s showed no sensitivity to the presence/absence of the filter within the pipeline and stayed equal to $f_s = 12.68\,\text{Hz}$.
3. The moment of the inlet recirculation inception was found to be uninfluenced by the filter body in all the test series but the case of $\alpha_{IG} = 60°$ when introducing a filter brought to a 4% TOA downshift of the recirculation onset.
4. The filter demonstrated the ability to damp the main surge fluctuation amplitude when installed. The damping rate, however, appeared to be dependent on the IGV positioning. The highest rate was unexpectedly recorded at $\alpha_{IG} = 60°$ by the gauge at impeller inlet and constituted 69%. Keeping IG opened ($\alpha_{IG} = 90°$) weakened the surge damping averagely up to 30% of amplitude. Closing the IG to $\alpha_{IG} = 30°$ neglected the damping at impeller inlet and even caused slight excitation of surge (up to 8%) downstream.

To provide a better understanding of the "filter-inlet guide vane-compression stage" system operation a more detailed study with a smaller α_{IG} changing step seems to be required and is planned to be a subject of further research.

REFERENCES

Fink D. A., Cumpsty N. A., Greitzer E. M., (1992), *Surge dynamics in a free-spool centrifugal compressor system, Journal of Turbomachinery*, 114, pp. 321–332

Fraser W. H., (1982), Recirculation in Centrifugal Pumps, World Pumps

Galerkin Y.B., (2010), Turbo compressors, KHT, Moscow (in Russian)

Harley P., Spence S., Filsinger D., Dietrich M., Early J, (2014), *Meanline modelling of inlet recirculation in automotive turbocharger centrifugal compressors*, The Proceedings of ASME TurboExpo 2014, GT2014-25853, Dusseldorf

Horodko, L., (2006), *Identification of rotating pressure waves in a centrifugal compressor diffuser by means of the wavelet cross-correlation*, International Journal of Wavelets, Multiresolution and Information Processing, 4(02), pp. 373-382.

Kabalyk K., Kryłłowicz W., (2013), *Conception for investigation the inlet damping phenomenon in a low speed single stage centrifugal blower*, 12th conference on Power System Engineering, Thermodynamics & Fluid Flow, Pilsen, Czech Republic.

Kabalyk K., Liskiewicz G., Horodko L., Stickland M., Kryllowicz W., (2014), *Use of Pressure Spectral Maps for Analysis of Influence of the Plenum Volume on the Surge in Centrifugal Blower*, The Proceedings of ASME TurboExpo 2014, GT2014-26931, Dusseldorf.

Koyama M., Komatsubara Y., Tsujita H., Mizuki S., (1998), *Effect of plenum volume on rotating stall and surge of centrifugal compressor*, Proceedings of ISROMAC-7, Honolulu, Hawaii, pp. 1159–1167

Kryłłowicz W., (2001), *Investigations of unstable operation of the single-stage radial compressor* (in Polish), Tech. Rep. 889, Technical University of Lodz

Liskiewicz G., Horodko L., Stickland M., Kryłłowicz W., (2014), *Identication of phenomena preceding blower surge by means of pressure spectral maps*, Experimental Thermal and Fluid Science, 54, pp. 267–278

Liśkiewicz G., Horodko L., (2014), *Time-frequency Analysis of the Surge Onset in the Centrifugal Blower*, 11th International Symposium on Compressor and Turbine Flow Systems Theory and Application Areas SYMKOM 2014 IMP2, Lodz, Poland, 20 - 23 October

Magiera R., Kryłłowicz W., (2006), *Wpływ zastosowania ciała centralnego w kierownicy wlotowej na strukturę przepływu przed kołem wirnikowym dmuchawy promieniowej*, (in Polish), Cieplne Maszyny Przepływowe CMP 130, pp. 107–116

Pampreen R., (1993), Compressor surge and stall, Concepts Eti, USA

Pfleiderer C., (1955), Die Kreiselpumpen fur Fleissigkeiten und Gase, Springer Verlag, Berlin-Gottingen-Heidelberg (in German)

Yedidiah S., (1996), Centrifugal Pump User's Guidebook, Chapman and Hall, New York